Journal of Bangladesh Academy of Sciences, Vol. 38, No. 1, 7-18, 2014

EFFECTS OF Li_2O ADDITIVE ON STRUCTURAL, MAGNETIC AND ELECTRICAL PROPERTIES OF Ni-Mg FERRITE

SHEIKH MOHI UDDIN RUMY, MAHABUB ALAM BHUIYAN*,
M. H. MESBAH AHMED, KAZI HANIUM MARIA, M. A. HAKIM[1],
D. K. SAHA[1] AND SHAMIMA CHOUDHURY

Department of Physics, University of Dhaka, Dhaka-1000, Bangladesh

ABSTRACT

The effects of Li_2O additives on the structural, magnetic and electrical properties of $Ni_{0.5}Mg_{0.5}Fe_2O_4$, prepared by conventional double sintering ceramic technique were investigated. The X-ray diffraction (XRD) pattern of the prepared samples showed single phase cubic spinel structure. Variation of lattice parameter has been observed with the variation of Li_2O content. The enhancement of bulk density has been observed for 2 mol% Li_2O additive, but further increase in Li_2O concentration, these values decrease. Enhancement of initial permeability (μ') have been observed for the sample with 2 mol% Li_2O additives while it decreases for higher concentration of Li_2O. The Curie temperature is found to decrease with the increase in Li_2O additive. The resistivity increases with increasing additive content and showed a significant dispersion with frequency, which is the normal ferromagnetic behavior. The dielectric constant (ϵ') measurement showed the normal dielectric behavior of spinel ferrite. Possible explanation for the observed features are discussed.

Key words: Microstructure, Permeability, Curie temperature, Resistivity, Dielectric constant

INTRODUCTION

The study of spinel ferrites is of great importance from both the fundamental and the applied research points of view and among them polycrystalline spinel ferrites are widely used in many electronic devices.

Most modern magnetically soft ferrites have spinel structure having chemical formula $MeFe_2O_4$, where 'Me' represents a divalent metal ion (e.g. Fe^{2+}, Ni^{2+}, Mg^{2+}, Mn^{2+}, Co^{2+}, Zn^{2+}, Cu^{2+}, etc.). Ferrites exhibit ferrimagnetism due to the super-exchange interaction between electrons of metal and oxygen ions. Due to the intrinsic atomic level interaction between oxygen and metal ions, ferrites have higher resistivity compared to ferromagnetic metals (Cullity 1972). This enables the ferrite to find applications at higher frequencies and makes it technologically very valuable. Along with this, the spinel type ferrites have tetrahedral A sites and octahedral B sites in AB_2O_4 crystal structure.

* **C**orresponding author: mail2mahabub@gmail.com>.
[1] Materials Science Division, Atomic Energy Centre, Dhaka-1000, Bangladesh.

Because of their crystal structure they show various magnetic properties depending on chemical composition and cation distribution in tetrahedral A sites and octahedral B sites (Hossain *et al.* 2007). Furthermore, various ions can be placed either at the tetrahedral A sites or octahedral B sites, which allows to control their magnetic properties.

Ni-Mg-Fe_2O_4 is very promising and draws many researchers attention due to its huge applications. These are supposed to be very good dielectric materials with low conductivity and have a wide field of technological applications in the range from microwave to radio frequencies. The electrical conduction and dielectric behavior of such ferrites markedly depend on the preparation conditions such as sintering temperature, chemical composition, the quantity and type of additives. Several investigations on the Ni-Mg-Fe_2O_4 have been reported in the literature (Hoffmann 1957, Faller and Birchenall 1970, El Hiti 1995, Kriessman and Harrison 1961) but the study of additives on Ni-Mg-Fe_2O_4 is inadequate. Therefore, one purpose of this investigation was to study the influence of different amounts of Li_2O on the ferrite structural, magnetic, transport properties and Curie temperature, considering that the Curie temperature of ferrites is primarily determined by the material's main prescription and crystal structure, and has little connection with the microstructure. However, the initial permeability, resistivity and dielectric constant are very sensitive to the materials' microstructre. So the authors studied the effects of adding Li_2O on Ni-Mg-Fe_2O_4 to improve the resistivity and permeability.

MATERIALS AND METHODS

NiO, MgO and Fe_2O_3 of high purity (99.9% and supplied by the manufacture E. Mark of Germany) were mixed homogeneously with appropriate ratio of cations and wet milled in a steel ball mill for 8 hrs. The samples were dried and the dried powder was pressed into disk shape. The disk shaped samples were pre-fired at 1000°C for 9 hrs in air to form ferrite through solid-state reaction. The presintered ferrite powder was crushed and mixed with 1 wt. % polyvinyl alcohol (PVA) as a binder and uniaxially pressed into toroid and pellets. The compacts were successively sintered in a programmable muffle furnace NAVER (Model-HT 08/16 Germany) in air at temperature 1300°C for 4.5 hrs to eliminate the PVA and finally furnace cooled to room temperature.

The spinel phase formation of the ferrite system was confirmed by X-ray diffraction patterns obtained by using CuKα radiation by PHILIPS (PW 3040) X Pert PRO X-Ray Diffractometer. The SEM micrographs have been studied by using a Scanning Electron Microscope (Inspect F50, EFI Company, Netherlands). Frequency dependence of permeability was measured up to 120 MHz. Temperature dependence permeability were measured by placing the samples in a tubular furnace according to the experimental setup described elsewhere from which Curie temperatures have been determined (Cedillo *et al.*

1980). Frequency dependent resistivity and dielectric constant (ϵ′) of the pellet samples has been measured up to 13 MHz by Wayne Kerr 3255 B Impedance Analyzer (Wayne Kerr Electronics Inc., Woburn, MA, USA).

RESULTS AND DISCUSSION

The structural study is essential for optimizing the properties needed for various applications. The phase identification and lattice parameters are determined by an X-ray diffractometer. The X-ray diffraction pattern of the prepared samples sintered at 1300^0C for 4.5 hrs are shown in Fig. 1. The patterns clearly show the formation of spinel structure for all samples and indicated that these materials have a well-defined single crystalline phase. By analyzing the XRD patterns it was observed that the peaks (220), (311), (222), (400), (511) and (440) comply with the reported value (Khan *et al.* 2013, Rath *et al.* 2002) and no traces of raw materials are found, thereby confirming that the chemical reaction is completed.

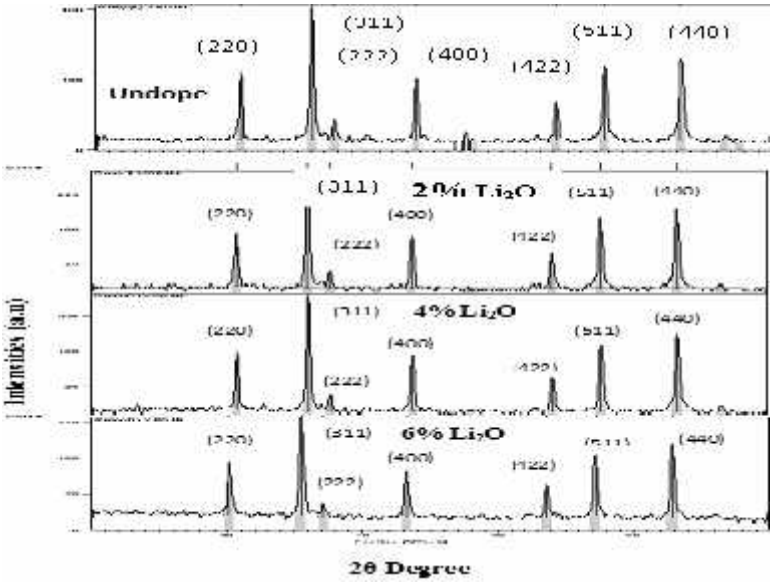

Fig. 1. XRD patterns of $NiMgFe_2O_4$ ferrites with Li_2O doping.

Using standard XRD data and Nelson-Riley function (Nelson and Riley 1945)

$$F(\theta) = \frac{1}{2}\left[\frac{\cos^2\theta}{\sin\theta} + \frac{\cos^2\theta}{\theta}\right] \quad (1)$$

lattice parameters were determined. The theoretical density, ρ_{th}, was calculated using the expression,

$$\rho_{th} = \frac{8M}{N_A a_o^3} \tag{2}$$

where N_A is the Avogadro's number, M is the molecular weight and a_o is the lattice constant. The porosity was calculated using the relation

$$P = \left(\frac{\rho_{th} - \rho_B}{\rho_{th}} \right) \times 100 \tag{3}$$

The lattice parameters, density and porosity of all samples are given in Table 1. From Table 1 it is observed that for the 2 mol% Li_2O doping, the lattice parameter is decreased. This may be attributed due to the replacement of larger cations Fe^{2+} (0.83 Å) by the smaller cations Li^{1+} (0.71 Å) (Goldman 2006, Bellad *et al.* 2000). Further addition of Li^+ the value of lattice parameter was expected to decrease. However, an increasing trend is observed. This shows that the lattice parameter does not solely depend on ionic radii. There may also be contributions from various factors like the long range attractive Coulomb forces, bond length, etc., calculation of which requires precise knowledge of shape and surface structure of the particles as well as existence of any surface charge (Sattar *et al.* 2007, Kotnala *et al.* 2010).

Table 1. The lattice parameters, theoretical density, bulk density and porosity of the prepared samples.

Sample Name	Lattice Parameter, a_0(Å)	Theoretical density, ρ_{th} (g/cc)	Bulk density, ρ_B (g/cc)	Porosity (%)
$Ni_{0.5}Mg_{0.5}Fe_2O_4$	8.353	4.95	4.497	9.33
+ 2 mol% Li_2O doped	8.342	5.00	4.529	9.13
+ 4mol% Li_2O doped	8.344	5.03	4.450	11.6
+ 6mol% Li_2O doped	8.346	5.07	4.246	16.2

Density plays an important role in controlling the properties of polycrystalline ferrites. The effects of Li_2O on the theoretical density (ρ_{th}), bulk density (ρ_B) and porosity (P) are shown in Table 1. From the table it is observed that the bulk density (ρ_B) is lower than the theoretical density (ρ_{th}). This may be due to the existence of pores which were formed and developed during the sample preparation or the sintering process.

From Table 1, it is also observed that ρ_{th} increases with the increase in Li_2O content because the molecular weight of the each sample increase significantly with the addition of Li_2O content. However, ρ_B increases with the increase in Li_2O up to 2 mol% and beyond this value it decreases. On the other hand, P of the samples has opposite trend. It is well known that the densification of ferrites is generally suppressed by the trapped pores within large grains followed by fast sintering process (Jeong and Han 2004). Here, the addition of small amounts of Li_2O (up to 2 mol%) efficiently increases the sintering

rate at 1300^0C, resulting in a bulk density of 4.529 gm/cm^3, which is a significant improvement, compared with the density of the specimen without the addition of Li_2O (4.497 gm/cm^3). But further addition of Li_2O, the density decreases. This may be attributed due to excess Li_2O bring fast sintering, resulting in an abnormal grain growth. Thus the fast sintering will leave some pores within large grains and inhibit the densification, which increases the porosity and are consistent with the scanning electron micrographs as shown in Fig. 2.

Microstructural analysis determines the average grain size and the type of grain growth of the samples, which influence the magnetic and electrical properties of the materials. The SEM micrographs of the prepared samples sintered at 1300^0C are shown in Fig. 2. From the micrographs it is observed that the grain size increases with the increase in Li_2O content up to 2 mol%. Beyond that addition of Li_2O, the structure becomes inhomogeneous and the abnormal grain growth occurs, which may be due to the fact that the Li^+ does not favor grain growth when present in excess amount.

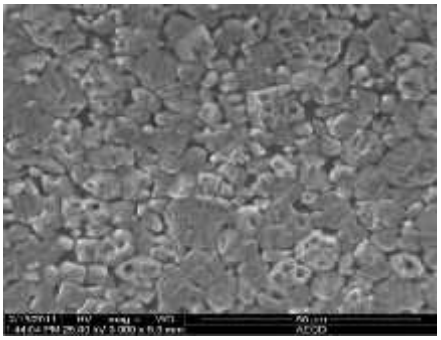

$Ni_{0.5}Mg_{0.5}Fe_2O_4$ (Undoped)

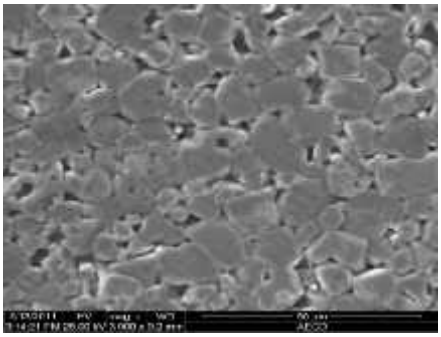

$Ni_{0.5}Mg_{0.5}Fe_2O_4$ with 2% Li_2O

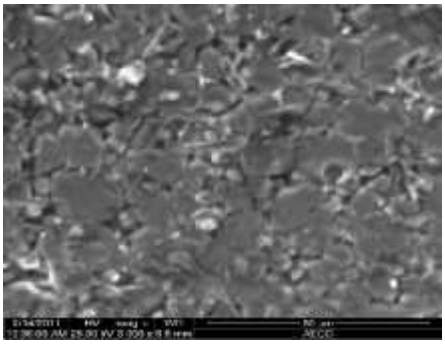

$Ni_{0.5}Mg_{0.5}Fe_2O_4$ with 4% Li_2O

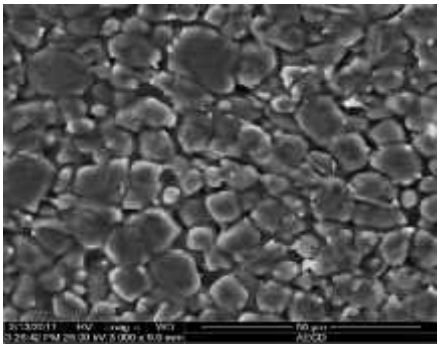

$Ni_{0.5}Mg_{0.5}Fe_2O_4$ with 6% Li_2O

Fig. 2. Scanning electron micrographs of prepared samples.

Fig. 3 represents the initial permeability (μ′) over the frequency range from 1 kHz to 120 MHz for the samples with different amount of Li_2O additives. The real part of the

initial permeability (μ′) represents the real permeability with the magnetization in phase with the alternating magnetic field. From Fig. 3 it is observed that the real part of the initial permeability (μ′) is fairly constant with frequency up to certain high frequency and then it decreases. The decrease in permeability implies onset of ferromagnetic resonance (Verma and Chatterjee 2006). The flat μ′ region up to the frequency where it starts declining rapidly gives the compositional stability and quality of prepared ferrite and is known as the zone of utility of the ferrite. And the higher stability of ferrites is a desirable characteristic for various applications such as broadband pulse transformation and wide band read-write heads for video recording etc.

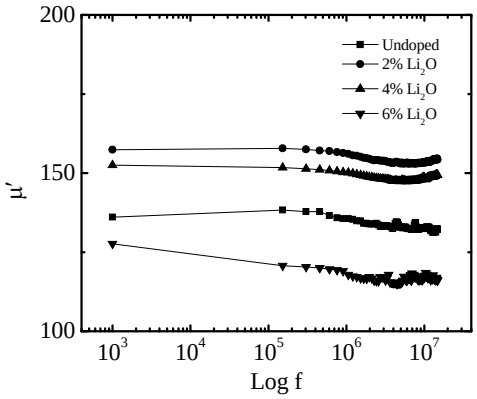

Fig. 3. Frequency dependent initial permeability (μ′).

It is also clear from Fig. 3 that the value of initial permeability (μ′) increased with the increase in Li_2O content at first and maximum for 2 mol% Li_2O over the frequency range studied. At Li_2O levels higher than 2 mol%, the value of μ′ decreased. The initial permeability is dependent on the chemical composition, microstructure, temperature, stress, time and several other factors after demagnetization. In general, the permeability is related to two different magnetization mechanisms of spin rotation and domain wall motion (Kumar *et al.* 1998). In small particles with a single domain, the domain wall motion is absent. Zaag *et al.* (1996) reported that particles larger than ~ 3 μm having multi-domain wall motion, made a contribution to the permeability. The density is also one of the most important factors leading to the high permeability, because pores inhibit the domain wall mobility and cause the demagnetization field (Shrotri *et al.* 1999). Thus, a densely sintered microstructure is essential for high permeability. For Li_2O content up to 2 mol%, the increase in permeability is in agreement with the grain size effect, while above 2 mol% Li_2O, larger grains include pores within grains and the pores hinder the magnetization process, resulting in lower permeability.

Curie temperature (T_C) is a basic quantity in the study of magnetic materials. It corresponds to the temperature at which a magnetically ordered material becomes

magnetically disordered, i.e. becomes paramagnet. Fig. 4 shows the variation of initial permeability with temperature for the prepared samples.

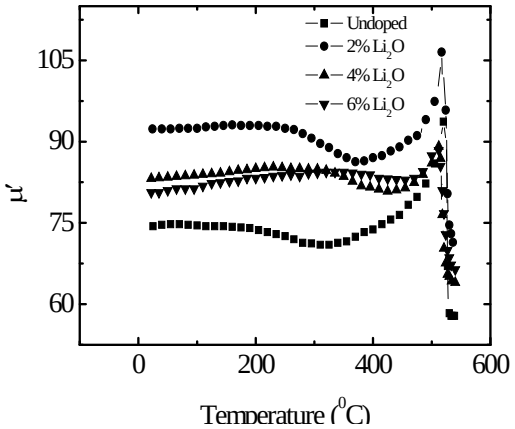

Fig. 4. Temperature dependent permeability.

It is seen that the initial permeability increased with temperature up to Curie temperature, T_C. This result could be explained according to the Globus relation (Globus *et al.* 1977), which is given by

$$\mu' = \frac{M_s^2 D}{\sqrt{©_1}} \tag{3}$$

where D is the average grain size, M_s is the saturation magnetization and $©_1$ is the anisotropy constant. The variation of μ' with temperature can be expressed as follows: the anisotropy constant ($©_1$) and saturation magnetization (M_s) usually decrease with increase in temperature. It is known that the anisotropy constant usually decreases much faster with temperature than saturation magnetization (Sumon *et al.* 2012, Mondal *et al.* 2012) which leads to increase in μ'. The maximum value of μ' just below the Curie temperature (T_C), is a manifestation of Hopkinson peak attributed to the minimization of anisotropy energy with temperature. Beyond this peak value μ′, initial permeability sharply falls to very low value indicating the ferro-paramagnetic phase transition. T_C has been taken as the temperature at which a sharp fall of permeability is observed i.e. where dμ'/dT attains its maximum value. The sharpness of the fall of pemeability indicates the homogeneity and the single phase of the studied samples, which have also been confirmed by X-ray diffraction (Globus and Monjaras 1975, Yellup and Parker 1979, Ghodake *et al.* 2006). No remarkable change in Curie temperature has been observed with the addition of Li_2O. Only a slight decrease in Curie temperature has been found with the increase in Li_2O content due to weakening of A-B interaction between the two

sublattices. This could be attributed to the increase in distance (hoping length, L) between the magnetic ions of tetrahedral A site (L_A) and the octahedral B sites (L_B) and is confirmed by the increase in the lattice parameter with increase in Li_2O content as shown in Table 1. The larger distance between magnetic cations leads to the decrease in A-B interaction and consequently lowered the Curie temperature.

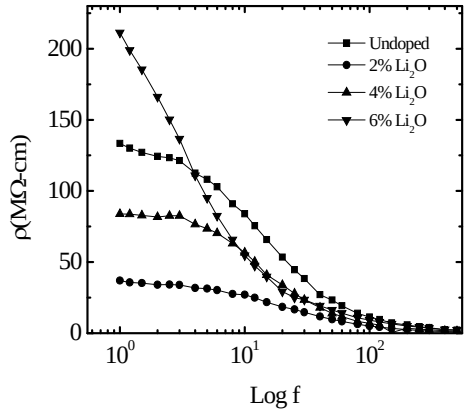

Fig. 5. Frequency dependent resistivity.

Fig. 5 shows the variation of AC resistivity with the log frequency at room temperature. All the samples show a significant dispersion with frequency, which is the normal ferromagnetic behavior. The conduction mechanism in ferrites is explained on the basis of hopping of charge carriers between the Fe^{2+} and Fe^{3+} ions on the octahedral site. The increase in frequency of the applied field enhances the hoping of charge carriers resulting in increase of conductivity and decrease of resistivity. At higher frequencies AC resistivity decreases and remains constant because of the fact that hopping frequency can no longer follow the frequency of the applied external field leading to lower values of AC resistivity. From Fig. 5, it is also clear that the resistivity is minimum for 2 mol % Li_2O addition but further increase in Li_2O content, the resistivity increases. These results are consistent with the microstructural results shown in Fig. 2. For the sample with 2 mol % Li_2O content has less pores but with the increase in Li_2O content, the pores increases. Since the pores are non conductive, the charge carriers will face more pores on their way with the increase in Li_2O content and thereby increase in resistivity.

Fig. 6 shows the variation of dielectric constant ϵ' with frequency at room temperature for all of the prepared samples. It can be seen from the Fig. 6 that the dielectric constant is found to decrease continuously with increasing frequency for all of the specimens exhibiting normal dielectric behavior of ferrites. The dielectric dispersion is rapid in the lower frequency region and remains almost independent at the high frequency region. The incorporation of Li_2O on the $Ni_{0.5}Mg_{0.5}Fe_2O_4$ has no pronounced

effect on the dielectric constant in high frequency, but significantly changes that in the low frequency range. The dielectric behavior of ferrites may be explained on the basis of the mechanism of the dielectric polarization process and is similar to that of the conduction process. The electronic exchange $Fe^{2+} \leftrightarrow Fe^{3+}$ give the local displacement of electrons in the direction of the applied electric field, which induces the polarization in ferrites (Kolekar *et al.* 1995). The magnitude of exchange depends on the concentration of Fe^{2+}/Fe^{3+} ion pairs present in the B site for the present ferrite. The sample with 2 mol% Li_2O content showed the maximum dispersion while that with 6 mol% Li_2O showed a least frequency dependence. The presence of Fe^{2+} ions in excess amount favors the polarization effects. Thus, the more dispersion observed in the sample with 2 mol% Li_2O can be attributed to the presence of Fe^{2+} ions in excess amount. Similarly, the weak dependence of dielectric constant on frequency in the samples with more Li_2O content can be due to the lack of Fe^{2+}/Fe^{3+} ions concentration. The observed decrease in dielectric constant with increase in frequency is due to the fact that above certain frequencies the electronic exchange between Fe^{2+}/Fe^{3+} ions does not follow the applied AC field.

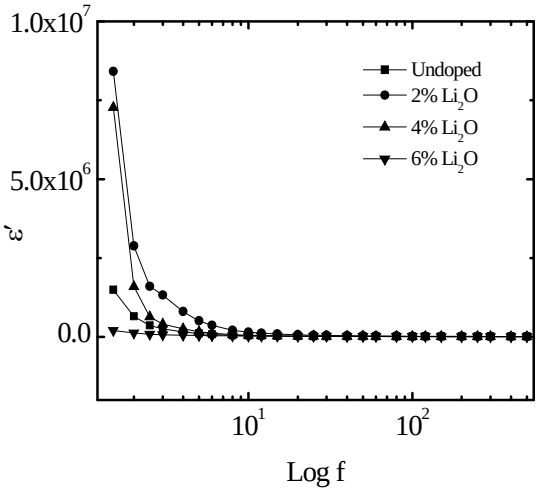

Fig. 6. Frequency dependent dielectric constant.

All samples have high values of ϵ′ in the order of 10^3-10^6 at low frequencies. This could be explained using Koop's phenomenological theory (Koops 1951), which was based on the Maxwell-Wagner model (Wagner 1913) for the inhomogeneous double layer dielectric structure. The dielectric structure was supposed to be composed of fairly well-conducting ferrite grains. These are separated by the second thin layer of grain boundaries which are poorly conducting substances. These grain boundaries could be formed during the sintering process due to the superficial reduction or oxidation of crystallites in the porous materials as a result of their direct contact with the firing

atmosphere (Reddy and Rao 1982). The grain boundaries of lower conductivity were found to be effective at lower frequencies while ferrite grains of high conductivity are effective at high frequencies (Koops 1951).This explains the higher values of ϵ′ at the lower frequencies and decrease in ϵ′ as the frequency increases.

According to Debye equation (Kingery *et al.* 1976),

$$£' = £_{\infty} + \frac{£_0 - £_{\infty}}{1 + \mu^{2} 2^{2}}$$

where, τ is the relaxation time, ϵ_0 the dielectric permittivity at a very low frequency and ϵ_∞ the dielectric permittivity at a very high frequency, respectively. This Debye equation indicates that ϵ′ decrease as the frequency increases. This is in agreement with the behavior of ϵ′ in the Fig. 6 for the present studied samples.

CONCLUSIONS

The XRD of all of the prepared samples showed single phase cubic spinel structure. The lattice parameters are found to decrease whereas the value of bulk density increases with the increase in Li_2O additives up to 2 mol%. But further increase in Li_2O contents, the lattice parameters increased and consequently the bulk density decreases, which are in agreement with the SEM micrographs. The value of initial permeability is maximum for 2 mol%Li_2O content but further increase in Li_2O content, the value of initial permeability decreased. Decrease in Curie temperature have been observed with the increase in Li_2O content which is due to the weakening of A-B exchange interaction between tetrahedral A sites and octahedral B sites. Both the resistivity and dielectric constant showed dispersion with the increase in frequency. It was also observed that the dielectric constant behaves in an opposite manner to that of electrical resistivity, giving an impression that both the dielectric constant ϵ′ and electrical conductivity (1/ρ) behave more or less in a similar way. As both the dielectric constant and electrical conductivity are basically electrical transport properties and their variation with additives' concentration is similar, it may be assumed that the same mechanism is responsible for both phenomena. These investigation clearly point towards the merits of the Li_2O additive for preparing NiMg ferrites with improved properties for many applications.

REFERENCES

Bellad, S. S., S. C. Watawe, A. M. Shaikh and B. K. Chougule. 2000. Cadmium substituted high permeability lithium ferrite. *Bull. Mater. Sci.* **23**(2): 83-85.

Cedillo, E., J. Ocampo, V. Rivera and R. Valenzuela. 1980. An apparatus for the measurements of initial magnetic permeability as a function of temperature. *J. Phys. E. Sci. Instrum.* **13**: 383-386.

Cullity, B. D. 1972. *Introduction to Magnetic Materials*. Addison-Wesley Publishing Company, Inc., California.

El Hiti, M. A. 1995. DC conductivity for $Ni_xMg_{1-x}Fe_2O_4$ ferrites. *J. Phase Transitions* **54**(2): 117-122.

Faller, J. G. and C. E. Birchenall. 1970. The temperature dependence of ordering in magnesium ferrite. *J. Appl. Cryst*. **3**: 496-503.

Ghodake, S. A., U. R. Ghodake, S. R. Sawant, S. S. Suryavanshi and P. P. Bakare. 2006. Magnetic properties of NiCuZn ferrites synthesized by oxalate precursor method. *J. Magn. Magn. Mater* **305:** 110-119.

Globus, A., H. Pascard and V. J. Cagan. 1977. Distance between magnetic ions and fundamental properties in Ferrites. *J. De Phys. Colloque* **38(4)**: 1.

Globus, A. and R. Monjaras. 1975. Influence of the deviation from stoichiometry on the magnetic properties of Zn-rich NiZn ferrites. *J. IEEE Trans. Mag.* **11(5)**: 1300-1302.

Goldman, A. 2006. *Modern Ferrite Technology*. Springer Science Media, Inc., Pittsburg, PA, USA.

Hoffmann, P.O. 1957. Magnetic and magnetostrictive properties of magnesium-nickel ferrites. *J. American Ceramic Society* **40(7)**: 250-252.

Hossain, A. K. M. A., S. T. Mahmud, M. Seki, T. Kawai and H. Tabata. 2007. Structural, electrical transport and magnetic properties of $Ni_{1-x}Zn_xFe_2O_4$. *J. Magn. Magn. Mater*. **312(1)**: 210-219.

Jeong, J. and Y. H. Han. 2004. Effect of Bi_2O_3 addition on the microstructure and electromagnetic properties of NiCuZn ferrites. *J. Materials Sci.: Materials in Electronics* **15**: 303-306.

Khan, A., M. A. Bhuiyan, G. D. Al-Quaderi, K. H. Maria, S. Choudhury, K. M. A. Hossain, S. Akther and D. K. Saha. 2013. Dielectric and transport properties of Zn-substituted cobalt ferrites. *J. Bangladesh Acad. Sci.* **37**(1): 73-82.

Kingery, W. D., H. K. Bowen and D. R. Uhlman. 1976. *Introduction to Ceramics*. 2nd edition, New York.

Kolekar C. B., P. N. Kamble, S. G. Kulkarni and A. S. Vaingankar. 1995. Effect of Gd^{3+} substitution on dielectric behavior of copper – cadmium ferrites. *J. Mater. Sci.* **30**: 5784-5788.

Koops, C., 1951. On the Dispersion of Resistivity and Dielectric Constant of Some Semiconductors at Audiofrequencies. *J. Phys. Rev.* **83:** 121-124.

Kotnala, R. K., M. A. Dar, V. Verma, A. P. Singh and W. A. Siddiqui. 2010. Minimizing of power loss in Li-Cd ferrite by nickel substitution for power applications. *J. Magn. Magn. Mater.* **322**: 3714-3719.

Kriessman, C. J. and S. E. Harrison. 1961. Cation distributions in magnesium-nickel ferrites. *J. Applied Physics* **32(3)**: 5392-5393.

Kumar, P. S. A., S. R. Sainkar, J. J. Shirotri, S. D. Kulkarni, C. E. Deshpande and S. K. Date. 1998. Particle size dependence of rotational responses in Ni–Zn ferrite. *J. Appl. Phys.* **83(11):** 6864-6866.

Mondal, S. P., K. H. Maria, S. S. Sikder, S. Choudhury, D. K. Saha and M. A. Hakim. 2012. Influence of annealing conditions on nanocrystalline and ultra-soft magnetic properties of $fe_{75.5}Cu_1Nb_1Si_{13.5}B_9$ alloy. *J. Mater. Sci. Technol*. **28(1):** 21-26.

Nelson, J. B. and D. P. Riley. 1945. An experimental investigation of extrapolation methods in the derivation of accurate unit-cell dimensions of crystals. *Proc. Phys. Soc. Lond*. **57:** 160.

Peelamedu, R., C. Grimes, D. Agrawal, R. Roy and P. Yadoji. 2003. Ultralow dielectric constant Nickel Zinc ferrites using microwave sintering. *J. Mater. Res.* **18**: 2292-2295.

Rath, C., S. Anand, R. P. Das, K. K. Sahu, S. D. Kulkami, S. K. Date and N. C. Mishra. 2002. Dependence on cation distribution of particle size, lattice parameter, and magnetic properties in nanosize Mn–Zn ferrite. *J. Appl. Phys.* **91(4):** 2211.

Reddy, P. V. and T. S. Rao. 1982. Dielectric behaviour of mixed Li-Ni ferrites at low frequencies. *J. Less-Common Metals* **86**: 255-261.

Sattar, A. A., H. M. El-Sayed, W. R. Agami and A. A. Ghani. 2007. Magnetic properties and electrical resistivity of Zr^{4+} substituted Li-Zn ferrite. *J. Am. Appl. Sci.* **4(2):** 89-93.

Shrotri, J. J., S. D. Kulkarni, C. E. Deshpande, A. Mitra, S. R. Sainkar, P. S. A. Kumar and S. K. Date. 1999. Effect of Cu substitution on the magnetic and electrical properties of Ni-Zn ferrite synthesised by soft chemical method. *J. Mat. Chem. Phy.* **59 (1)**: 1-5.

Sumon, K. N., K. H. Maria, S. Noor, S. S. Sikder, S. M. Hoque and M. A. Hakim. 2012. Magnetic ordering in Ni-Cd ferrite. *J. Magn. Magn. Mater*. **324**: 2116-2120.

Verma, A. and R. Chatterjee. 2006. Effect of zinc concentration on the structural, electrical and magnetic properties of mixed Mn-Zn and Ni-Zn ferrites synthesized by the citrate precursor technique. *J. Magn. Magn. Mater.* **306:** 313-320.

Wagner, K. 1913. Zur Theorie der Unvolkommenen Dielectrika. *J. Ann. Phys.* **40**: 817.

Yellup, J. M. and B. A. Parker. 1979. The determination of compositions in nonhomogeneous ferromagnetic materials by Curie temperature measurements. *J. Phys. Sta. Sol.* ***A***. **55:** 137-145.

Zaag, P. J. V. D., P. J. V. D. Valk and M. Th. Rekveldt. 1996. A domain size effect in the magnetic hysteresis of NiZn- ferrites. *J. Appl. Phys. Lett.* **69**: 2927-2929.

(*Received revised manuscript on 1 December, 2013*)